Supplementary Information

Materials and Methods

DNA Plasmids, Cell Culture and Reagents

FAK biosensor was recently developed based on FRET(1). The FAT-FAK biosensor is created in pcDNA3.1 by fusing a PCR product of FAT domain with KpnI and EcoRI sites at the C-terminus of the cytosolic FAK biosensor. FAK mutant FRNK was previously described(2). KAKTLRK mutant(3, 4) and the wild-type FAK plasmid(5) are kind gifts from Prof. Michael D. Schaller at West Virginia University and Prof. Margaret C. Frame at University of Edinburgh, UK, respectively. KAK-EDQ and WT-EDQ mutants were created by generating mutations on E158A/D161A/Q162A in KAKTLRK mutant or wild-type FAK plasmid, using the QuickChange method (Stratagene). FAT-PTP was constructed in pcDNA3.1 plasmid by fusing Shp2 PTP domain and FAK FAT domain, which were amplified by PCR. Shp2 constitutively active mutant (Shp2 CA) in pcDNA3.1 including the D61Y mutation was generated by the QuickChange method. HT1080, MDA-MB-231, and U87-MG cells were cultured with Dulbecco's modified Eagle medium (DMEM) supplemented with 10% fetal bovine serum (FBS), 2 mM L-glutamine, 1 unit/ml penicillin, 100 μg/ml streptomycin, and 1 mM sodium pyruvate. Cells were maintained in a humidified 95% air, 5% CO_2 incubator at 37°C. Cell culture reagents were purchased from Invitrogen. Lipofectamine 2000 (Invitrogen) was used for the transfection of plasmids.

Fibronectin from bovine plasma (FN) was purchased from Sigma, and type-I collagen from rat tail (Col I) was purchased from BD Biosciences. Poly-D-Lysine (PDL), Cytochalasin D (CytoD) and ML7 were obtained from Sigma. Y-27632 was purchased from Calbiochem.

Antibodies and Peptides

Integrin activating antibodies SNAKA51 (α5 activating antibody), mAb11 (α5 control antibody), 12G10 (β1 activating antibody), and 12G10 mAb were previously described(6). The β1 control antibody, K20, was purchased from Santa Cruz Biotechnology. Anti-integrin α2β1 antibody, anti-integrin β1 antibody, anti-integrin α2 and anti-integrin α5 antibodies were obtained from Millipore. Integrin antibodies for FACS analysis were obtained from BD Biosciences. GFOGER peptide and FNIII7-10 were previously described(7). RGD peptide was from Peptide International. CPHSRN and CHPRNS peptides were synthesized by LifeTein.

Preparation of Polyacrylamide Gels with Coupled ECM Proteins

Polyacrylamide gels were prepared as previously described(8). Briefly, 40% w/v acrylamide and 2% w/v bis-acrylamide stock solutions (Bio-Rad) were combined to prepare polyacrylamide gel solution. Gels with different stiffness were obtained by varying the final concentrations of polyacrylamide solution (3%, 3%, 5.5%, and 7.5%) and bis-acrylamide cross-linker (0.04, 0.06, 0.08, and 0.4%) for the corresponding stiffness of 0.2, 0.6, 2, and 40 kPa(9). To polymerize the solutions, 2.5 μl of 10% w/v ammonium persulfate (Bio-Rad) and 0.25 μl of N,N,N9,N9-tetramethylethylenediamine (TEMED; Bio-Rad) were added to yield a final volume of 500 μl polyacrylamide solution. To cross-link extracellular matrix proteins onto the gel surface, sulfo-SANPAH (sulfosuccinimidyl-6-(4'-azide-2'-nitrophenyl-amino) hexanoate, Pierce) was applied and coupled with 200 μl of 0.1 mg/ml fibronectin solution (from bovine plasma, Sigma) or type-I collagen (from rat tail, Sigma) at 37°C for overnight..

Traction Force Measurement

The details of traction force measurement have already been described elsewhere(10). In brief, cells were cultured on polyacrylamide gels with red fluorescent beads (0.2 μm in diameter) embedded in the top surface of the gel. Fluorescent images of the beads before and after trypsinization of the cells were captured and the displacement of the beads in the two images was computed using a MATLAB code. The traction field was then calculated from the displacement field using an established method(11).

Bead Coating

The beads with carboxyl surface groups (Spherotech, 4.44 um in diameter) were incubated with 1-ethyl-3-[3-dimethylaminopropyl] carbodiimide hydrochloride (EDC, 10 mg/ml) and N-hydroxy-succinimide (NHS, 10 mg/ml) in MES buffer [50 mM 2-(N-morpholino) ethanesulfonic acid, 100 mM NaCl, pH 5.0] for 15 min at room temperature with constant mixing to activate the surface carboxyl groups. The beads were then centrifuged at 12,000 rpm for 15 min and the supernatant removed. GFOGER peptide or Poly-D-Lysine (PDL) were added at 25, 75, or 150 μg per mg bead and incubated with beads in coupling buffer (HEPES 20 mM, 100 mM NaCl, 5 mM $CaCl_2$, pH 8.0) for 2 hr with continuous mixing at room temperature. The activated carboxyl groups on beads can covalently bind free amine groups on the protein. Quenching buffer (100 mM Tris, 20 mM NaCl, 5 mM $CaCl_2$, pH 8.0) was added to stop the reaction. Free proteins were removed by centrifuging the beads and removing the supernatant.

Immunoprecipitation and Immunoblotting

To examine the binding between FAK and myosin, different FAK constructs (wild-type and mutants) were transfected in HT1080 cells. After 36 hr of transfection, cell lysates were subjected

to immunoprecipitation with an anti-FAK antibody (sc558, Santa Cruz Biotechnology) to pull down the FAK proteins, followed by the immunoblotting with an anti-myosin heavy chain antibody (Millipore) or with an anti-FAK antibody as a control band. The intensity of the band was calculated by ImageJ program.

Image Acquisition

Cells were cultured in cover-glass-bottom dishes (Cell E&G) and maintained in CO_2-independent medium containing 0.5% FBS (Gibco BRL) at 37°C during imaging. Images were collected by a Zeiss Axiovert microscope and MetaFluor 6.2 software (Universal Imaging) with a 420DF20 excitation filter, a 450DRLP dichroic mirror, and two emission filters controlled by a filter changer (475DF40 for ECFP and 535DF25 for YPet). The excitation filter for ECFP at 420 ± 20 nm was selected to shift toward lower wavelength away from the peak excitation spectra of ECFP to reduce the cross-excitation of YPet and hence the effect of bleed-through on the FRET channel. The fluorescence intensity of non-transfected cells was quantified as the background signal and subtracted from the ECFP and YPet signals of transfected cells. The pixel-by-pixel ratio images of ECFP/YPet were calculated based on the background-subtracted fluorescence intensity images of ECFP and YPet by using the MetaFluor software. These ratio images were displayed in the intensity modified display (IMD) mode in which the color and brightness of each pixel is determined by the ECFP/YPet ratio and ECFP intensity, respectively.

Supplementary Figure Legends

Figure S1. The design of the FRET-based FAK biosensor

(**A**) The FAK biosensor is composed of ECFP, SH2 domain derived from c-Src, a flexible linker, a substrate peptide, and YPet. The substrate peptide is derived from FAK containing Tyr397

(indicated as red Y). Active FAK can phosphorylate the substrate peptide in the FAK biosensor, which subsequently binds to the intramolecular SH2 domain to cause a FRET decrease. FAK activity can be represented by ECFP/YPet emission ratio. (**B**) The tyrosine phosphorylation level of the FAK biosensor in MEF cells after adhesion on the FN-coated surface for the indicated time period without or with FAK inhibitor PF228. The tyrosine phosphorylation level and total amount of the biosensors, which were immunoprecipitated by an anti-GFP antibody from MEF cells, were detected by an anti-phosphotyrosine (pY20) and anti-GFP antibody, respectively.

Figure S2. FN interacts with integrin α5β1 in HT1080 cells.

(**A**) The representative DICIII image of HT1080 cells applied on FN-coated polyacrylamide gels with different rigidity without or with the incubation of inhibitory antibody for integrin α5β1 or αvβ3. (**B** and **C**) The average ECFP/YPet ratio of FAK biosensor in HT1080 cells on different stiffness gels treated with inhibitory antibody for integrin α5β1 (N=3 and 7) (**B**) or αvβ3 (N=7 and 12) (**C**). Graphs show mean ± SEM. * represents a significant difference ($P<0.05$). Scale bar=10 μm.

Figure S3. FAK activity can be modulated by actomyosin-derived intracellular tension.

The representative ECFP/YPet ratio images of FAK biosensor and mCherry-tagged paxillin in H1080 cells seeded on FN-coated glass surface with the treatment of 1 μM of CytoD (**A**) or 10 μM of ML7 (**B**) for different periods of time as indicated (N=20). Scale bar=10 μm.

Figure S4. The disruption of actomyosin-derived tension caused an earlier reduction of traction force than the decrease of FAK activity.

(**A** and **B**) Time courses of the average ECFP/YPet ratio of FAK biosensor (**A**) and traction (**B**) in response to 10 μM of ML7 with colored lines indicating the values and times for 25% (blue), 50% (red), or 100% (green) reduction of overall changes. The ECFP/YPet ratio and traction were normalized by the average values before the treatment of ML7. (**C**) Average time (min) to reach the reduction level of 25%, 50%, and 100% of overall changes of FAK activity (black bars) or traction (white bars) after ML7 treatment were compared with students' t-test (N=7). * represents a significant difference ($P<0.05$). Graphs show mean ± SEM.

Figure S5. Intracellular tension-dependent FAK activity at focal adhesions

(**A**) The FAT-FAK biosensor is created by fusing a FAT domain targeting at focal adhesion sites to the C-terminus of the cytosolic FAK biosensor. (**B**) The representative ECFP/YPet ratio images of FAT-FAK biosensor in HT1080 cells seeded on FN-coated glass surface and treated by 10 μM of ML7 for different periods of time as indicated. Scale bar=10 μm. Peripheral focal adhesions in the white dotted box are enlarged in the lower panels.

Figure S6. Focal adhesion structures of HT1080 cells seeded on polyacrylamide gels are weak.

Focal adhesions in HT1080 cells seeded on FN- or Col I-coated 0.6 kPa or 40 kPa gels were highlighted by mCherry-tagged paxillin. Scale bar=10 μm.

Figure S7. FAK activation is dependent on substrate rigidity coupled with fibronectin (FN), but not with type-I collagen (Col I).

(**A**) The phosphorylation levels at FAK Y397 on 0.6 kPa and 40 kPa gels were quantified using western blotting. The total FAK expression level was detected by anti-FAK antibody. (**B**) The

difference in the ECFP/YPet ratio of membrane raft-targeted Lyn-FAK biosensor(1) in and outside of focal adhesions were compared. The FAK activity difference was significantly decreased by the treatment of 10 mM of PF228, a specific FAK inhibitor. (**C**) The average ECFP/YPet ratios of Lyn-FAK biosensor seeded on 0.6 kPa or 40 kPa gels coupled with FN or Col I (N=15-21). Graphs show mean ± SEM. * represents a significant difference ($P<0.05$).

Figure S8. Different FAK mechanoactivations on FN or Col I in MDA-MB-231 and U87-MG cells.

(**A**) The averaged ECFP/YPet ratio values of FAK biosensors in MDA-MB-231 cells adhered on 0.6 kPa or 40 kPa gels coated with FN or Col I (N=11-22). (**B**) The average ECFP/YPet ratio of FAK biosensors in MDA-MB-231 cells applied to FN-coated 40 kPa gels or Col I-coated 0.6 kPa gels, with or without 10 μM of ML7 for 1 hr (N=15-20). (**C**) The average ECFP/YPet ratio of FAK biosensors in the suspended MDA-MB-231 cells with or without 40 μg/ml of Col I treatment (N=15-21). (**D** and **E**) The ECFP/YPet ratio of FAK biosensors in U87-MG cells applied on (**D**) FN- or (**E**) Col I-coated PA gels of different stiffness. (N=35-68) (**F**) The average ECFP/YPet ratio of FAK biosensors in the suspended U87-MG cells with or without 40 μg/ml of Col I treatment (N=44, 63). * represents a significant difference ($P<0.05$). Graphs show mean ± SEM.

Figure S9. GFOGER peptide cannot induce FAK activation in suspension.

(**A**) The average ECFP/YPet ratio values of FAK biosensor in the suspended HT1080 cells upon the incubation with different concentrations of GFOGER peptide in the presence of 40 μg/ml of Col I (N=20). The ECFP/YPet ratio of each group was normalized by the value of suspension group without any treatment. (**B**) The representative images of FAK biosensor in the suspended

HT1080 cells upon the incubation with different concentrations of Col I. (**C**) The average ECFP/YPet ratio values of FAK biosensor with different dosage of Col I (N=24-50) or GFOGER peptide (N=24-34). * represents a significant difference ($P<0.05$). Graphs show mean ± SEM. Scale bar=10 μm.

Figure S10. FAK cannot be activated by FN or FN fragments in suspended cells.

The average ECFP/YPet ratio values of FAK biosensor in the suspended HT1080 cells after the incubation of different concentrations of FN (**A**), FNIII7-10 domains (**B**), or RGD peptides (**C**) (N=18-31). The ECFP/YPet ratio of each group was normalized by the value of control suspension group without any treatment. Graphs show mean ± SEM.

Figure S11. The comparable expression levels of integrin α2 and α5 in HT-1080 cells.

(A) The total expression levels of integrin α2 and α5 on the FN- and Col I-coated surface quantified by western blotting. The band intensity was quantified by ImageJ. (B) The surface levels of integrin α2 and α5 in suspended cells measured by FACS analysis. (C) The representative immunostaining images of integrin α2 on Col I and α5 on FN. The fluorescence intensity of peripheral regions was quantified using ImageJ and the averaged values (mean ± SEM) of each group were compared with students' t-test. (N=30).

Figure S12. FAK can be activated by integrin β1 activating antibody.

(**A**) The average ECFP/YPet ratio values of FAK biosensor in the suspended HT1080 cells after the incubation with 10 μg/ml of 12G10 or 12G10 mAb (N=20-26). The ECFP/YPet ratio of each group was normalized by the value of control suspension group without any treatment. Graphs

show mean ± SEM. * represents a significant difference ($P<0.05$). (**B**) The histogram of cell populations with different ECFP/YPet ratios of FAK biosensors in HT1080 cells adhered on 0.6 kPa gels coated with 12G10 (100 μg/ml).

Figure S13. The phosphorylation of Y397 is required for the FAK activation, which is maintained by Shp2 and FERM-PIP_2 interaction during cell adhesion.

(**A**) The average ECFP/YPet ratio values of FAK biosensor in cells without (black) or with the expression of Shp2 constitutively active mutant (Shp2 CA) (dark grey) or Shp2 PTP (protein tyrosine phosphatase) domain fused to FAT domain targeting at focal adhesions (light grey). (N=9-14). Graphs show mean ± SD. (**B**) The average ECFP/YPet ratio values of FAK biosensor in cells without (black) or with the expression of KAKTLRK mutant (white) during cell adhesion on the Col I-coated glass surface. (**C**) The average ECFP/YPet ratio values of FAK biosensor in HT1080 cells treated by 0.5 mM of neomycin. * represents a significant difference ($P<0.05$). Graphs show mean ± SEM.

Figure S14. The FERM basic patch/PIP_2 interaction is required to maintain the FAK activity from inhibitory myosin II during cell adhesion.

(**A**) The structure of FAK FERM and Kinase domains. The EDQ acidic sites and KAKTLRK basic patch in FERM domain are highlighted with red and blue color, respectively. Y397 is indicated with orange color. The cleft in FERM, which was suggested to bind to myosin (12), and active loop (A-loop) in Kinase domain are also highlighted. (**B** and **C**) The schematic model of the regulatory mechanisms of the (**B**) KAKTLRK and (**C**) KAK-EDQ mutants of the FAK molecule.

Movie S1. FAK activity and focal adhesion dynamics in response to CytoD.

Movie of the ECFP/YPet ratio images of FAK biosensor and mCherry-tagged paxillin in H1080 cells seeded on FN-coated glass surface with the treatment of 1 μM of CytoD. The ECFP/YPet ratio ranges from 0.6 to 1.0.

Movie S2. FAK activity and focal adhesion dynamics in response to ML7.

Movie of the ECFP/YPet ratio images of FAK biosensor and mCherry-tagged paxillin in H1080 cells seeded on FN-coated glass surface with the treatment of 10 μM of ML7. The ECFP/YPet ratio ranges from 0.65 to 1.25.

References

1. Seong J, *et al.* (2011) Detection of focal adhesion kinase activation at membrane microdomains by fluorescence resonance energy transfer. *Nat Commun* 2:406.
2. Wu X, Suetsugu S, Cooper LA, Takenawa T, & Guan JL (2004) Focal adhesion kinase regulation of N-WASP subcellular localization and function. *J Biol Chem* 279(10):9565-9576.
3. Dunty JM, *et al.* (2004) FERM domain interaction promotes FAK signaling. *Mol Cell Biol* 24(12):5353-5368.
4. Cai X, *et al.* (2008) Spatial and temporal regulation of focal adhesion kinase activity in living cells. *Mol Cell Biol* 28(1):201-214.
5. Serrels B, *et al.* (2010) A complex between FAK, RACK1, and PDE4D5 controls spreading initiation and cancer cell polarity. *Curr Biol* 20(12):1086-1092.
6. Clark K, *et al.* (2005) A specific alpha5beta1-integrin conformation promotes directional integrin translocation and fibronectin matrix formation. *J Cell Sci* 118(Pt 2):291-300.
7. Reyes CD, Petrie TA, & Garcia AJ (2008) Mixed extracellular matrix ligands synergistically modulate integrin adhesion and signaling. *J Cell Physiol* 217(2):450-458.
8. Kim TJ, *et al.* (2009) Substrate rigidity regulates Ca2+ oscillation via RhoA pathway in stem cells. *J Cell Physiol* 218(2):285-293.
9. Yeung T, *et al.* (2005) Effects of substrate stiffness on cell morphology, cytoskeletal structure, and adhesion. *Cell Motil Cytoskeleton* 60(1):24-34.
10. Wang N, *et al.* (2002) Cell prestress. I. Stiffness and prestress are closely associated in adherent contractile cells. *Am J Physiol Cell Physiol* 282(3):C606-616.
11. Butler JP, Tolic-Norrelykke IM, Fabry B, & Fredberg JJ (2002) Traction fields, moments, and strain energy that cells exert on their surroundings. *Am J Physiol Cell Physiol* 282(3):C595-605.
12. Santos AM, *et al.* (2011) FERM domain interaction with myosin negatively regulates FAK in cardiomyocyte hypertrophy. *Nat Chem Biol* 8(1):102-110.

Supplementary Figure S1

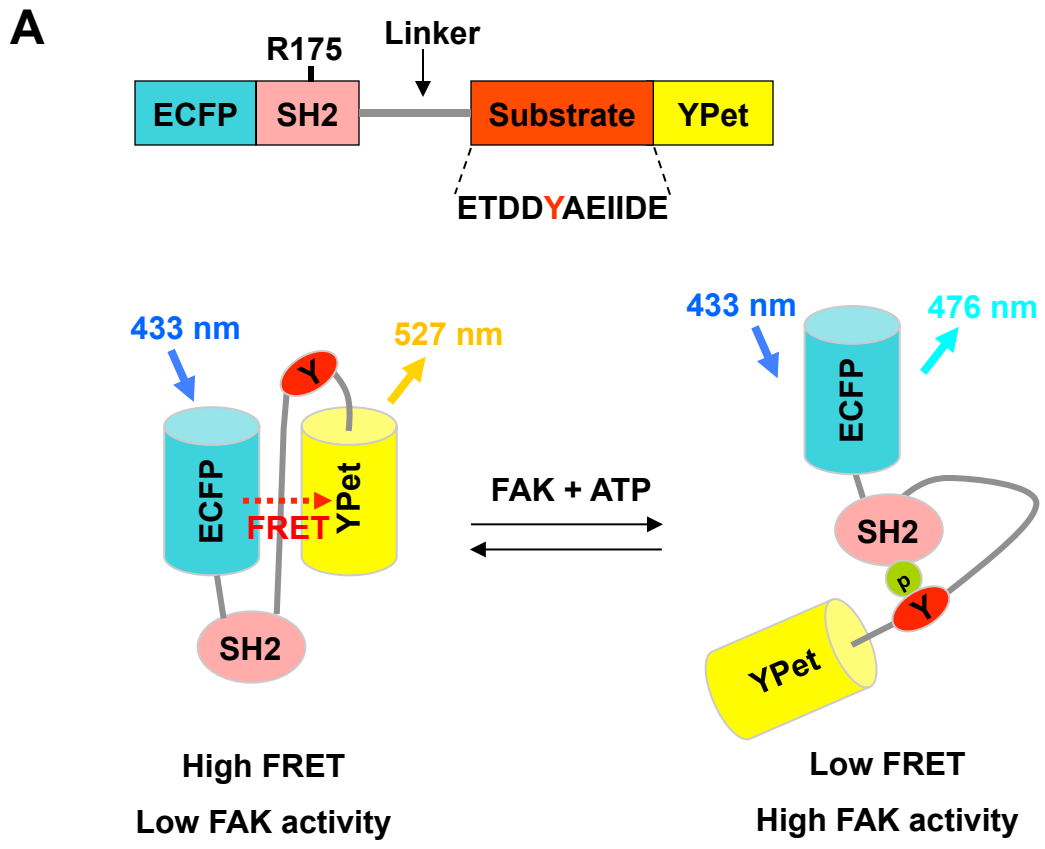

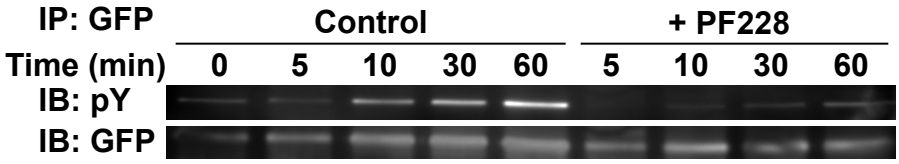

Supplementary Figure S2

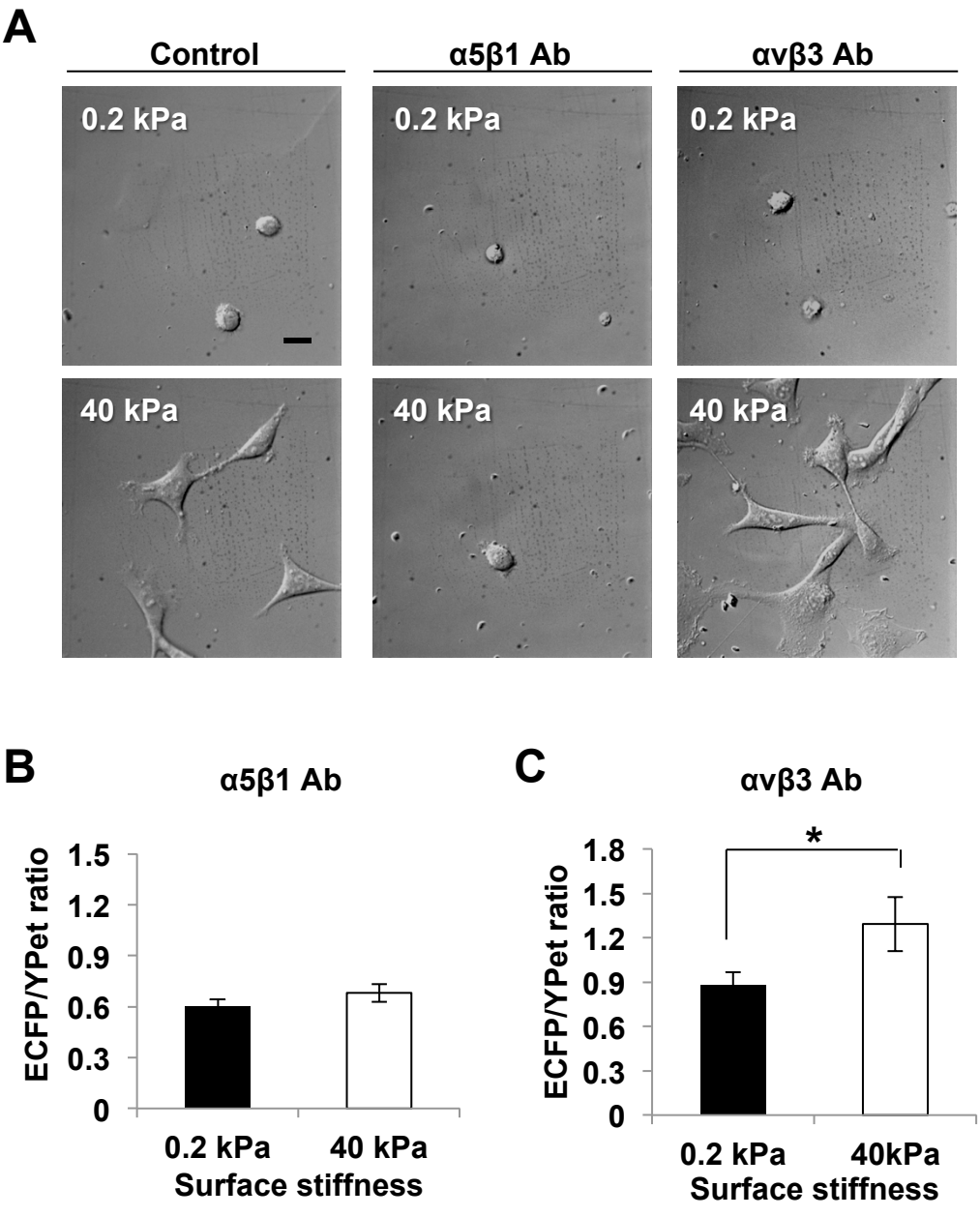

Supplementary Figure S3

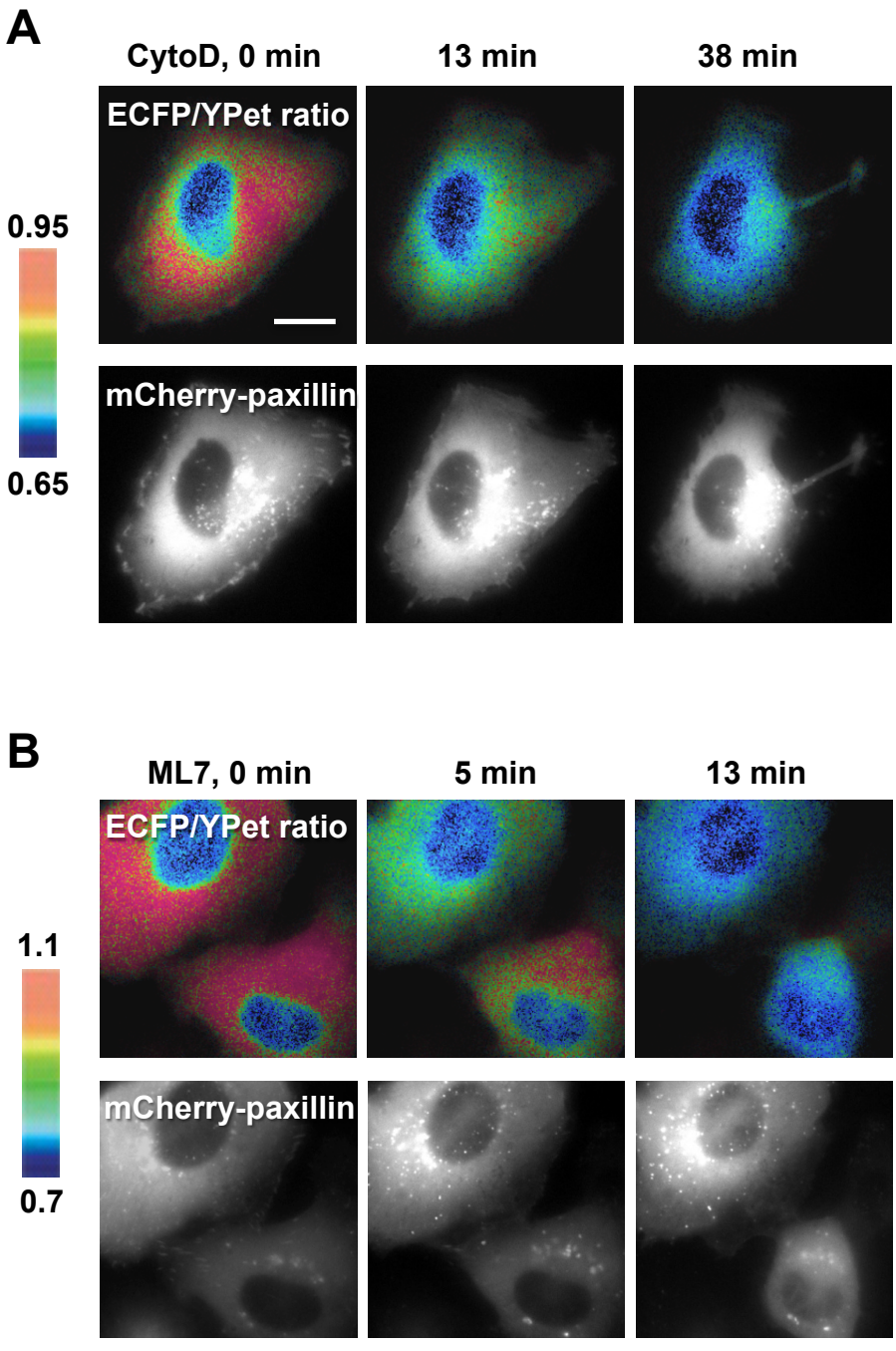

Supplementary Figure S4

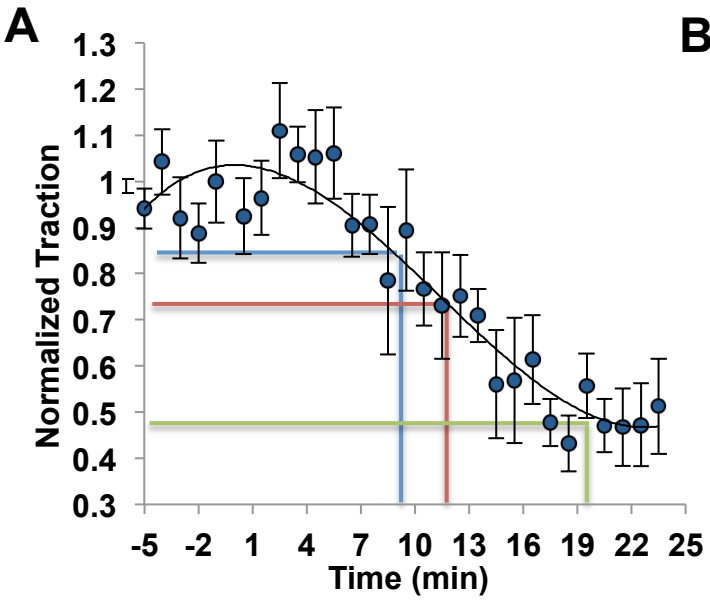

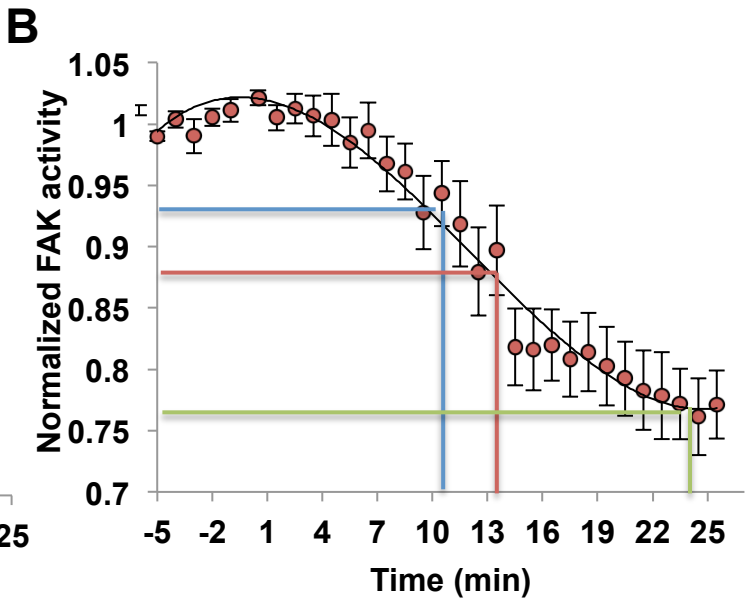

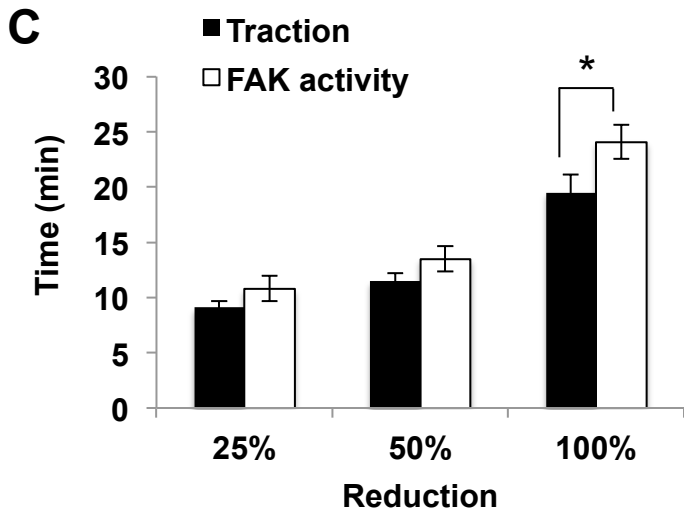

Supplementary Figure S5

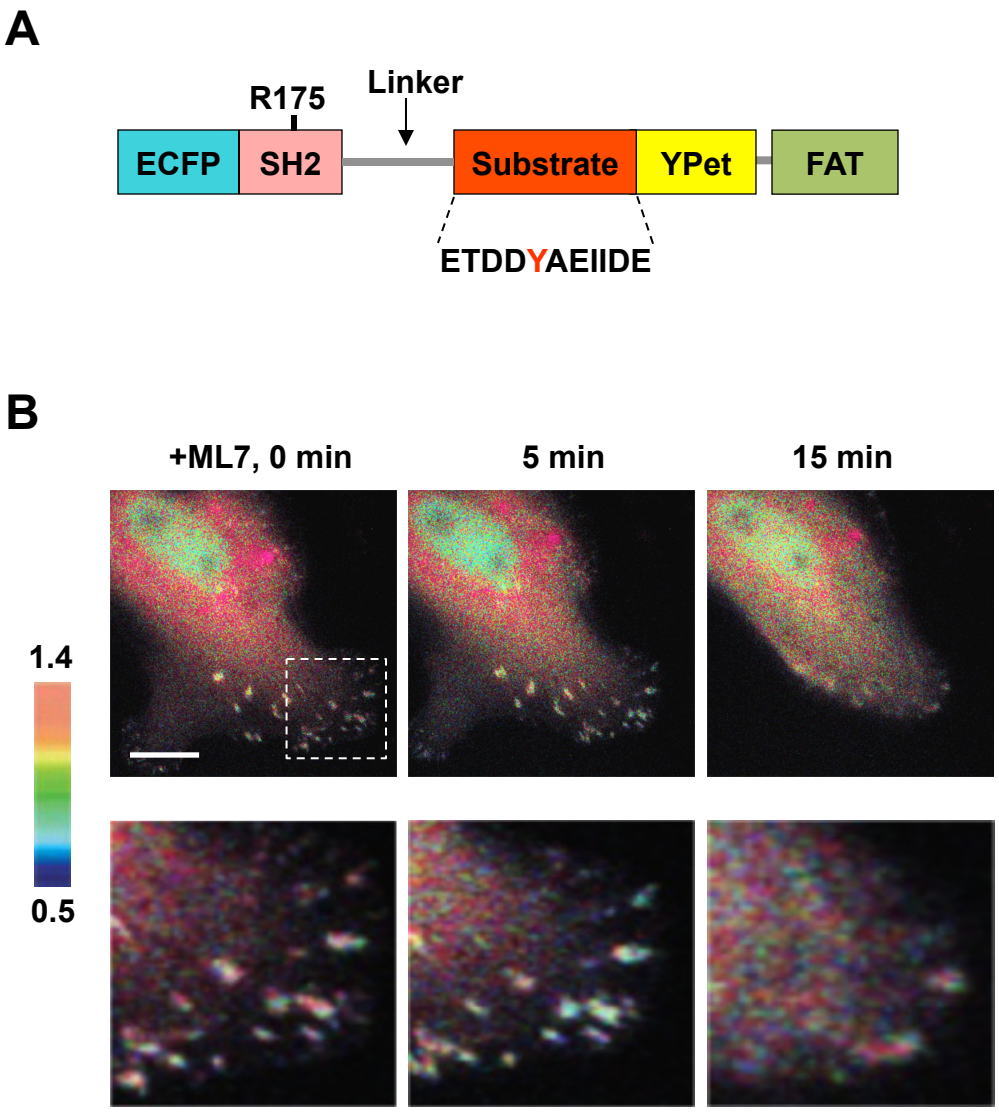

Supplementary Figure S6

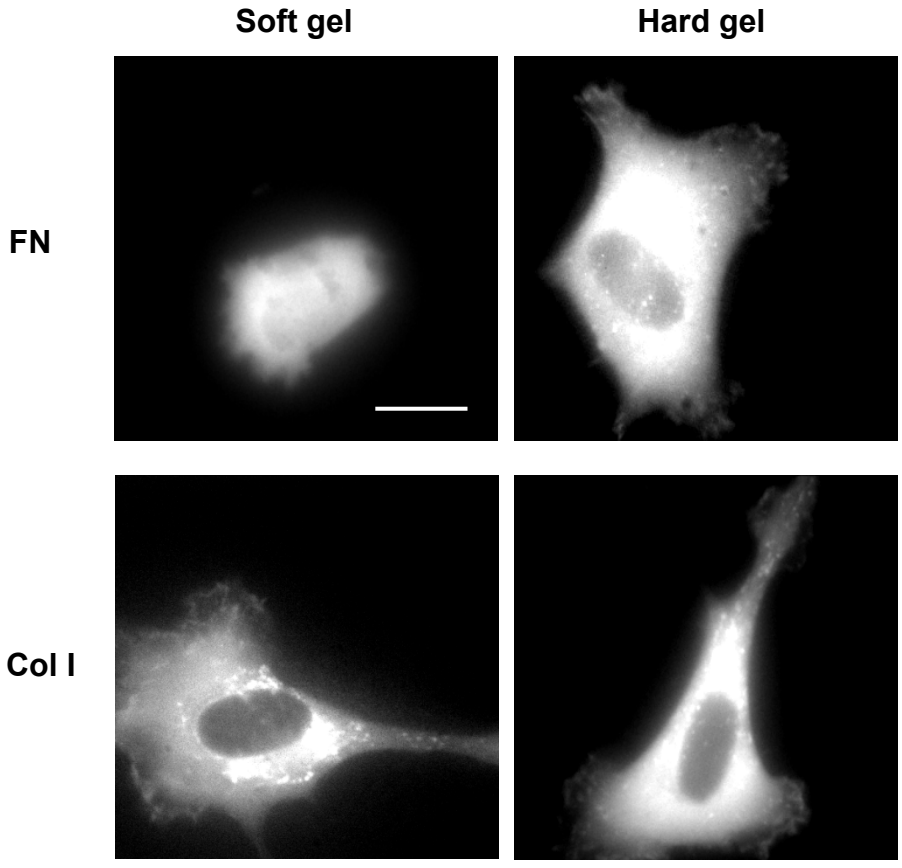

Supplementary Figure S7

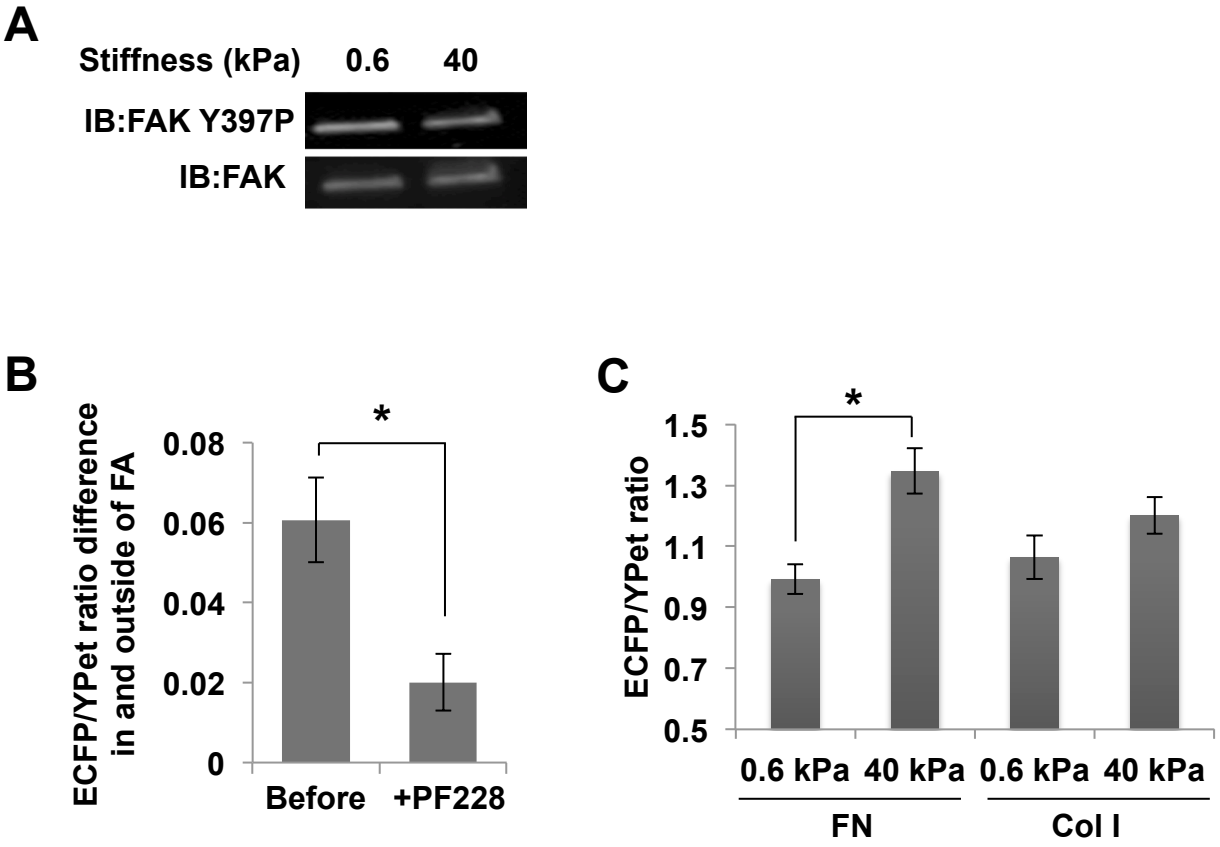

Supplementary Figure S8

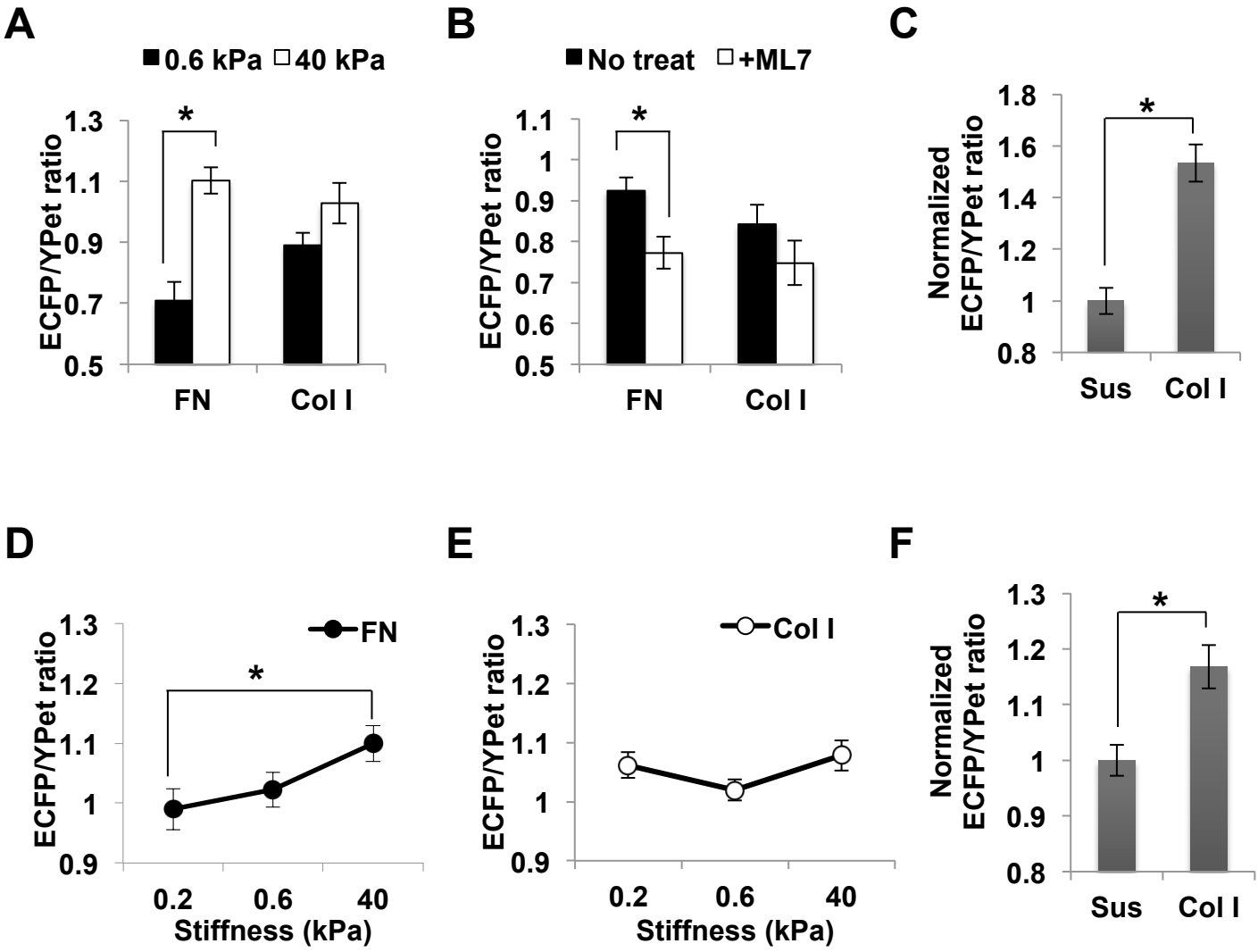

Supplementary Figure S9

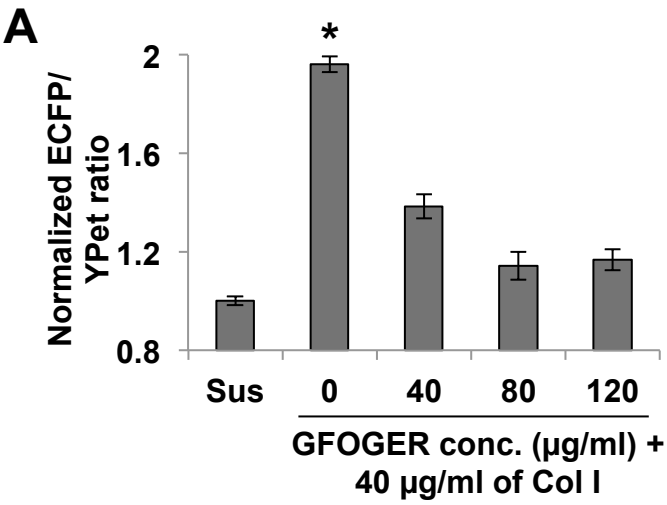

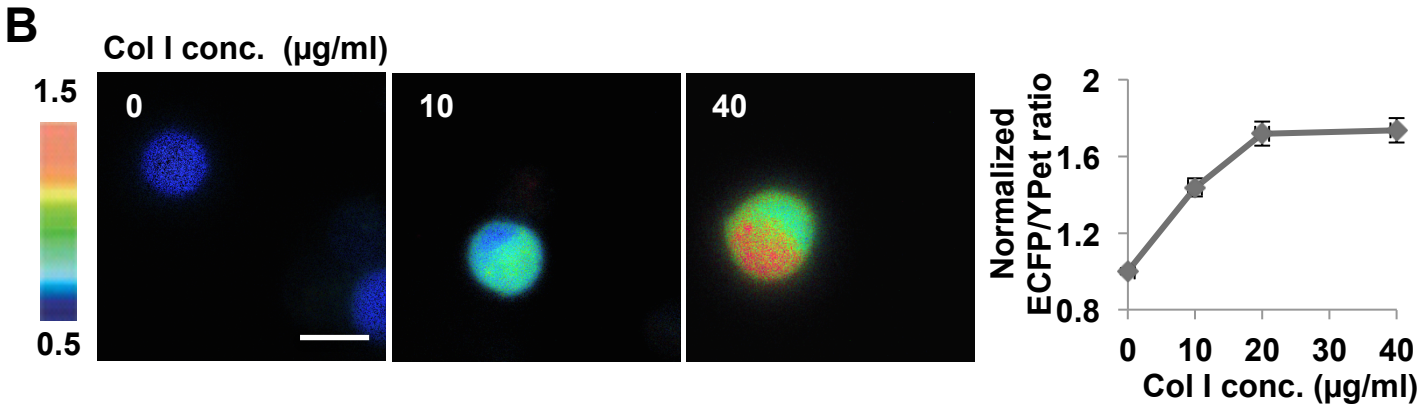

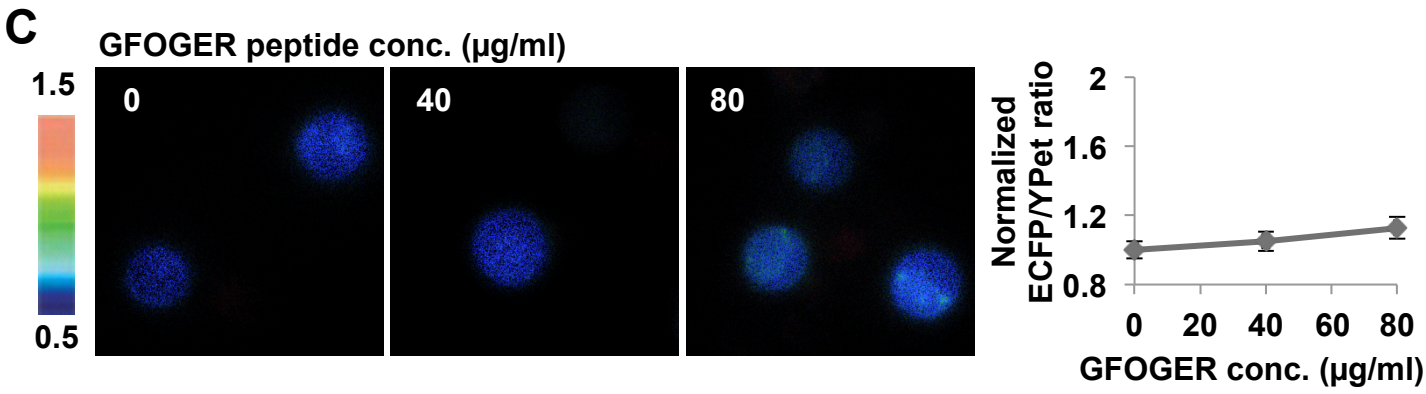

Supplementary Figure S10

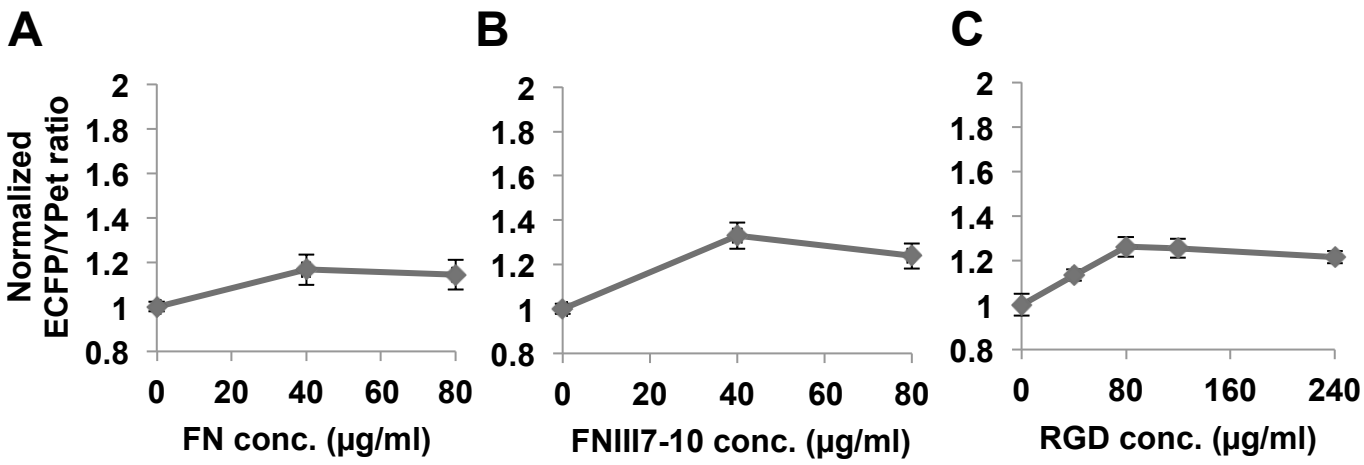

Supplementary Figure S11

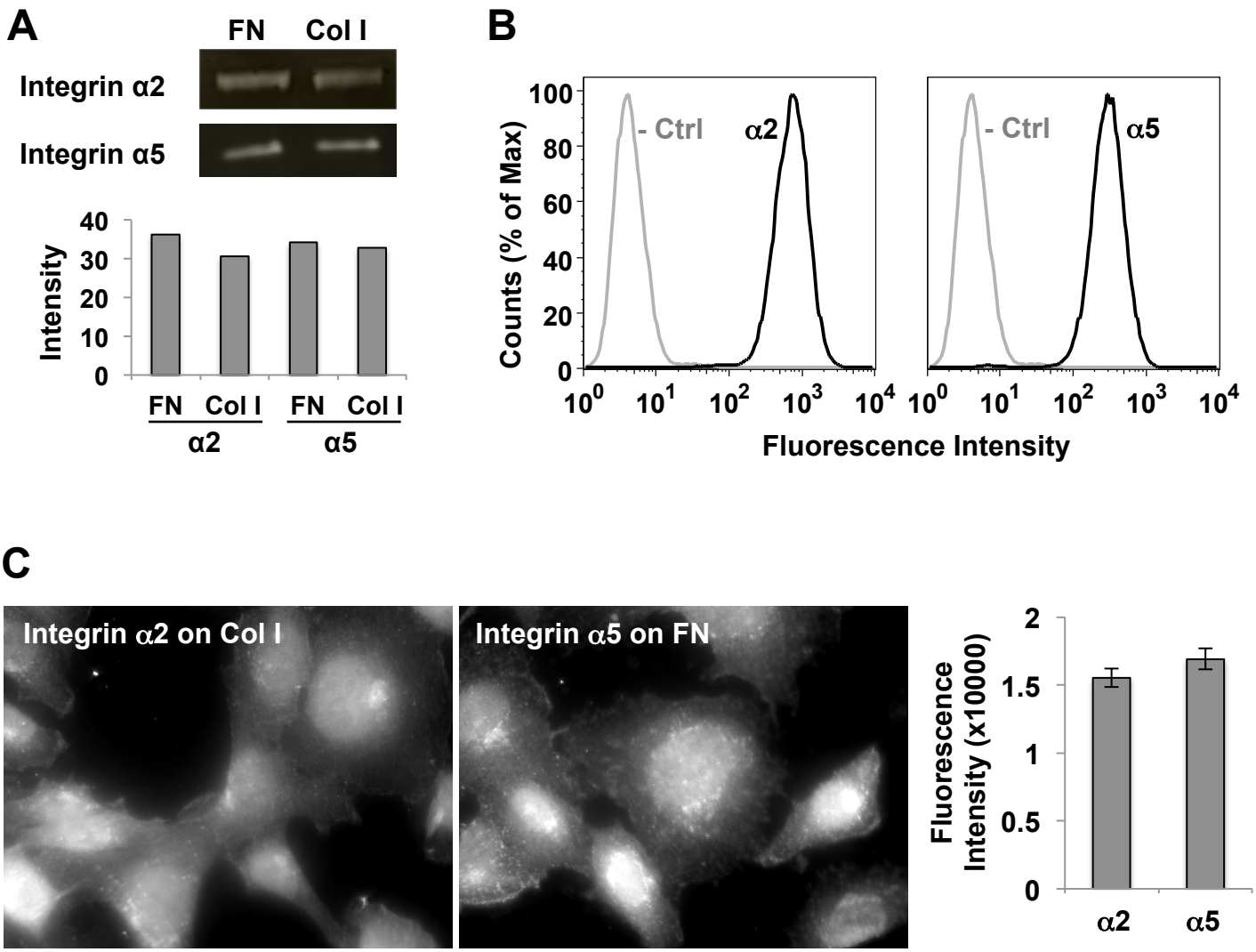

Supplementary Figure S12

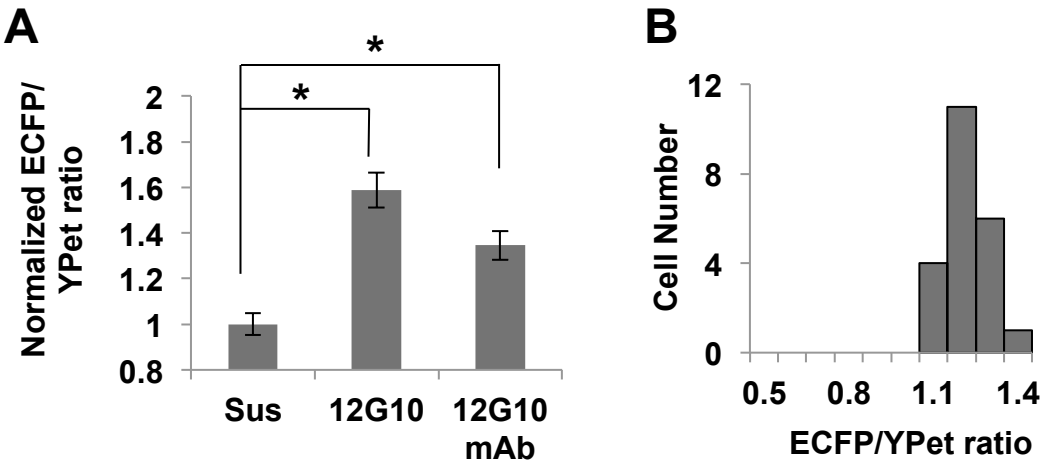

Supplementary Figure S13

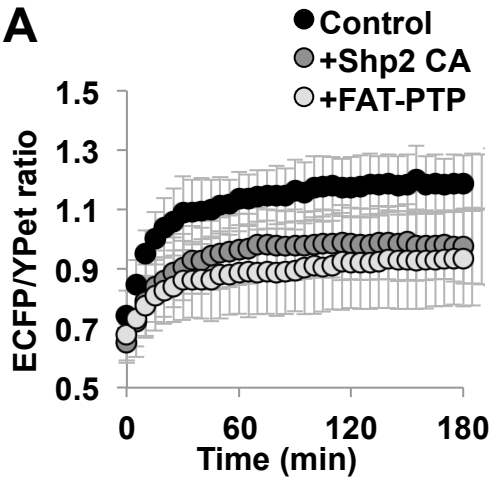

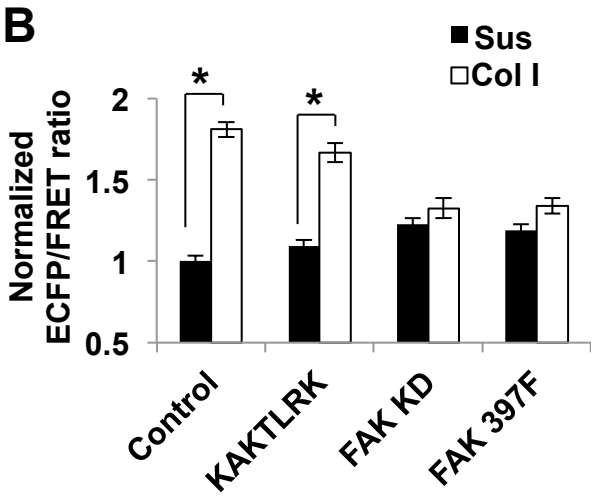

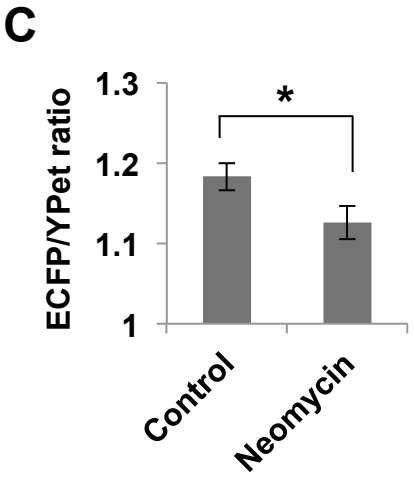

Supplementary Figure S14